









## Technology of reducing greenhouse gas emissions for decarbonization and decreasing anthropogenic pressure on the environment

S. Bolegenova , A. Askarova , Sh. Ospanova\* ,  
S. Zhumagaliyeva , A. Makanova ,  
A. Aldiyarova , A. Nurmukhanova  and G. Idrissova 

Physics and Technology Department, Al-Farabi Kazakh National University, Almaty, Kazakhstan

\*e-mail: [Shynar.Ospanova@kaznu.edu.kz](mailto:Shynar.Ospanova@kaznu.edu.kz)

(Received April 28, 2024; received in revised form May 13, 2024; accepted May 17, 2024)

The focus of this article is to research technology for reducing greenhouse gas emissions, such as carbon dioxide and nitrogen, produced by internal combustion engines when liquid fuels are burned in them to minimize humans' negative impact on the environment. Based on statistical data, the work presents an analysis of the dynamics of local and global emissions into the atmosphere in recent years and preventive measures to reduce them for decarbonization. The mathematical model is based on basic conservation equations that explain the liquid fuels combustion process in high turbulence. The paper outlines the outcomes of computational experiments that were carried out to determine the best conditions for the combustion of liquid fuels (petrol and heptane). The droplet injection rate in the combustion chamber at high turbulence was analyzed to determine the atomization and combustion processes. Optimum combustion parameters for petrol and heptane were identified. The temperature and dispersion characteristics of the fuel-air mixture, along with the concentration fields of combustion products such as CO<sub>2</sub> and N<sub>2</sub>, and the aerodynamics of multiphase flow for two types of liquid fuels were determined through computational experiments. The optimum combustion modes for petrol and heptane were determined based on the attained results, which can facilitate rational fuel combustion, reduce the number of released harmful emissions, and enhance engine efficiency. Implementing the optimum parameters that were achieved for the combustion of hydrocarbon liquid fuels in the combustion chambers of actual heat engines will minimize the anthropogenic load on the surrounding atmosphere with the release of greenhouse gases, promote decarbonization in the energy sector, and reduce the carbon footprint.

**Key words:** combustion, liquid fuels, decarbonization, greenhouse gases, harmful emissions.

**PACS number(s):** -47.70.Fw.

### 1 Introduction

Global environmental threats are greatly exacerbated by air pollution. The International Labour Organization defines air pollution as the presence of dangerous or harmful substances in the air without specifying their physical form. Fossil fuel combustion, agriculture, and mining are just some of the factors that contribute to air pollution. The air pollutants that are most prevalent and substantial include carbon dioxide, sulfur dioxide, nitrogen oxides, and dust.

Most countries around the world have always been concerned about carbon dioxide emissions. This is because the increase in the amount of gas

produced has serious consequences for the climate and the environment. The effects are so severe and broad that they involve modifications to climate conditions, increases in ocean levels, melting glaciers, unpredictability of precipitation, and even depletion of the ozone layer.

The complex global picture of carbon dioxide emissions in 2023 reflects the ongoing struggle between economic development and environmental sustainability. The entire global community will still be affected by global CO<sub>2</sub> emissions even as awareness increases and efforts are made to transition to cleaner energy sources in 2023. Emissions trends indicate a need for urgent action to address climate change, with both setbacks and

progress seen this year. The greenhouse effect is amplified by the accumulation of CO<sub>2</sub> and other greenhouse gas emissions in the atmosphere, which traps heat and causes global temperatures to rise. This warming contributes to climate change by affecting ecosystems, weather patterns, sea levels, and overall environmental sustainability [1-3].

According to the International Energy Agency, global energy CO<sub>2</sub> emissions rose by 1.1% in 2023 to reach a new record high of 37.4 billion tonnes. The electricity and heat generation sector recorded the largest increase in emissions. Emissions from the electricity and heat sector increased by 1.8% to a historic high of 14.7 billion tonnes. The main reason for this increase was the switch from gas to coal in many regions, which led to a 2.1 percent increase in CO<sub>2</sub> emissions from coal-fired power generation [4].

A complex global scenario with record high levels and regional differences is evident in the analysis of carbon dioxide emissions in 2023, resulting in urgent action to combat climate change. To keep global temperatures under control, the EU has pledged to achieve a 55 percent reduction in

greenhouse gas emissions by the decade apex compared to 1990 levels and to reach "net zero" by 2050. According to the report of the European Scientific Advisory Council on Climate Change, the 27 Member States need to reduce emissions about twice as fast as they have been doing so on average over the past 17 years.

Kazakhstan's atmosphere in 2023 is heavily polluted by sulfur dioxide, nitrogen oxides, carbon oxides, ammonia, and hydrogen sulfide. From the total volume of pollutants emitted into the atmospheric air, 80.7 percent were gaseous and liquid substances and 19.3 percent were solid substances (Fig.1) [5, 6].

Decarbonization is the process of replacing fossil fuel-based systems with electricity that is produced using low-carbon resources such as renewable energy. Traditional energy sources such as coal, oil, and natural gas cannot be abandoned due to our current level of technology. Nonetheless, it is already possible to boost the effectiveness of their utilization to decrease emissions. Climate stabilization cannot be achieved without the energy system's complete decarbonization.

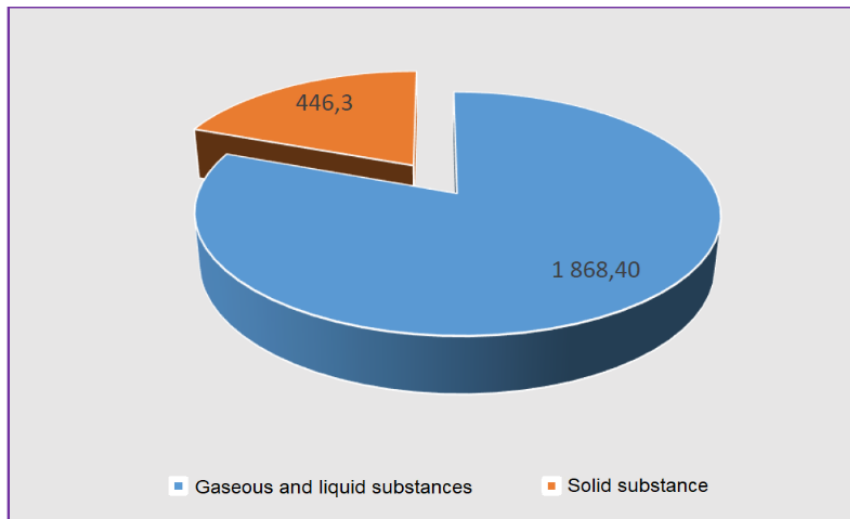


**Figure 1** – Emissions of pollutants into the air by consistency for 2023, thousand tons

Low-carbon energy sources are used to reduce carbon dioxide emissions by decarbonization, which results in reducing greenhouse gas emissions. The global economy should be completely decarbonized by 2050, carbon taxes must be introduced, and adaptation to climate change must be stepped up by

the international community [7, 8]. Despite this, carbon dioxide emissions are still on a plateau and are rapidly rising. The idea of carbon neutrality and zero emissions means that the number of emissions produced is not greater than the carbon engrossed by forests and oceans.

Scientific and technological progress is accompanied by an increase in environmental pollution, which can change its indicators and parameters. Under these conditions, it is necessary to study the impact of various pollutants on the environment, assess possible negative environmental consequences, and relying on the outcomes of the assessment, if necessary, implement local or global measures to prevent them promptly [9].

The increase in carbon dioxide emissions and its concentration in the air changes the functioning of the carbon cycle that has developed over the centuries and, together with other gases, the greenhouse effect on the Earth, which has a general tendency to increase, causing climate warming.

It is very important to establish the scientific basis for an intensive technological process that integrates the use of fuels and their wastes and eliminates the detrimental effects of their production on the biosphere. The present-day methodology of nature security and energy sparing infers the choice of the foremost successful accomplishments of scientific and innovative advance, among which three fundamental bunches of measures are highlighted: utilization, energy modernization, and accelerated energy sparing. In this respect, and the light of the Euro natural benchmarks rules, it is essential to move forward the quality of internal combustion motors, which in turn are controlled by the liquid fuel injection framework.

## 2 Mathematical model of liquid particles spray and combustion in a reacting flow

Equations of fluid phase motion, droplet evaporation, energy, and mass transfer with appropriate initial and boundary conditions determine the mathematical representation of liquid fuel atomization and combustion [10-16].

The  $m$  component's continuity equation is written in the following manner [10-13]:

$$\begin{aligned} \frac{\partial \rho_m}{\partial t} + \bar{\nabla}(\rho_m \bar{u}) = \\ = \bar{\nabla} \left[ \rho D \bar{\nabla} \left( \frac{\rho_m}{\rho} \right) \right] + \dot{\rho}_m^c + \dot{\rho}_m^s \delta_{m1}, \end{aligned} \quad (1)$$

where  $\rho_m$  is the  $m$  component's mass density,  $\rho$  is the full mass density, and  $u$  is fluid velocity. The

liquid's continuity equation (1) can be obtained by summing the equation of the overall phases.:

$$\frac{\partial \rho}{\partial t} + \bar{\nabla}(\rho \bar{u}) = \dot{\rho}^s. \quad (2)$$

The liquid phase's momentum transfer equation is expressed in this way [11, 12]:

$$\begin{aligned} \frac{\partial(\rho \bar{u})}{\partial t} + \bar{\nabla}(\rho \bar{u} \bar{u}) = \\ = -\frac{1}{a} \bar{\nabla} p - A_0 \bar{\nabla} \left( \frac{2}{3} \rho k \right) + \bar{\nabla} \bar{\sigma} + \bar{F}^s + \rho \bar{g}, \end{aligned} \quad (3)$$

where the laminar flows have a zero value of  $A_0$ , and turbulent flows have a unity value of  $A_0$ .

The following formula describes the viscous stress tensor [11]:

$$\sigma = \mu \left[ \bar{\nabla} \bar{u} + (\bar{\nabla} \bar{u})^T \right] + \lambda \bar{\nabla} \bar{u}. \quad (4)$$

Droplet spraying requires phase transformations to maintain the law of conservation of internal energy [13]:

$$\begin{aligned} \frac{\partial(\rho \bar{I})}{\partial t} + \bar{\nabla}(\rho \bar{u} \bar{I}) = -\rho \bar{\nabla} \bar{u} + \\ + (1 - A_0) \bar{\sigma} \bar{\nabla} \bar{u} - \bar{\nabla} \bar{J} + A_0 \rho \varepsilon + \dot{Q}^c + \dot{Q}^s. \end{aligned} \quad (5)$$

The relation is responsible for determining the heat flux vector  $J$  [9, 14]:

$$\bar{J} = -k \bar{\nabla} T - \rho D \sum_m h_m \bar{\nabla}(\rho_m / \rho), \quad (6)$$

where  $T$  is liquid temperature,  $h_m$  is the  $m$  component's enthalpy,  $\dot{Q}^c$  is used to describe the heat produced by a chemical reaction,  $\dot{Q}^s$  is the amount of heat that fuel injection brings.

Models with two differential equations are more flexible in engineering calculations of turbulent flows. The model with two differential equations is the most frequently used one in technical flows. In this  $k - \varepsilon$  model, the kinetic energy of turbulence and its dissipation rate are solved through the use of two equations. [15, 16]:

$$\rho \frac{\partial k}{\partial t} + \rho \frac{\partial \bar{u}_j k}{\partial x_j} = \frac{\partial}{\partial x_j} \left[ \left( \mu + \frac{\mu_t}{\sigma_k} \right) \frac{\partial k}{\partial x_j} \right] \frac{\partial \bar{u}_i}{\partial x_j} + G - \frac{2}{3} \rho k \delta_{ij} \frac{\partial \bar{u}_i}{\partial x_j} - \rho \varepsilon, \quad (7)$$

$$\rho \frac{\partial \varepsilon}{\partial t} + \rho \frac{\partial \bar{u}_j \varepsilon}{\partial x_j} - \frac{\partial}{\partial x_j} \left[ \left( \mu + \frac{\mu_t}{\sigma_\varepsilon} \right) \frac{\partial \varepsilon}{\partial x_j} \right] = c_{\varepsilon_1} \frac{\varepsilon}{k} G - \left[ \left( \frac{2}{3} c_{\varepsilon_2} - c_{\varepsilon_3} \right) \rho \varepsilon \delta_{ij} \frac{\partial \bar{u}_i}{\partial x_j} \right] - c_{\varepsilon_2} \rho \frac{\varepsilon^2}{k}. \quad (8)$$

These are standard  $k - \varepsilon$  equations. The model's simplicity, good convergence, and accuracy make it the most used model for modeling a wide range of turbulent flows. The popularity of this turbulence model is due to its simplicity, cost-effectiveness, and accurate prediction of the properties of both non-reacting and burning flows. The model can be successfully used to calculate the characteristics of a reacting flow with chemical transformations due to its ability to work well at high Reynolds numbers and high flow turbulence. The experiment has led to the determination of model constants  $c_{\varepsilon_1}$ ,  $c_{\varepsilon_2}$ ,  $c_{\varepsilon_3}$ ,  $\sigma_k$ ,  $\sigma_\varepsilon$  [17]. The empirical determination of standard values for these constants is commonly used in engineering calculations.

### 3 Physical statement of the problem and computing mesh

A quantitative assessment of harmful anthropogenic gaseous emissions emitted during heat engine operation has been conducted by computer studies of the combustion processes of two kinds of liquid hydrocarbon fuels in combustion chambers. The following fuels were used in this work: petrol and heptane. Carbon dioxide and water are produced by the combustion of these fuels in the combustion chamber.

Petrol is the fuel used most frequently in cars. Automobile and motorcycle engines use automotive petrol as fuel, and it can also be used to make engine components for other purposes. The colorless liquid known as petrol is a mixture of hydrocarbons of different structures and can boil at a temperature of 33-205°C. It is employed in vehicles designed for

both cargo and passengers, as well as individual motor vehicles.

The liquid heptane, which is colorless and flammable, is used as rocket fuel and has a low flash point of around 4°C and a high auto-ignition temperature of 223°C. Heptane vapors in air have an area of ignition that is 1.1-6.7 % (by volume). Heptane is a hydrocarbon from the paraffin series and is categorized as a hazardous substance [18].

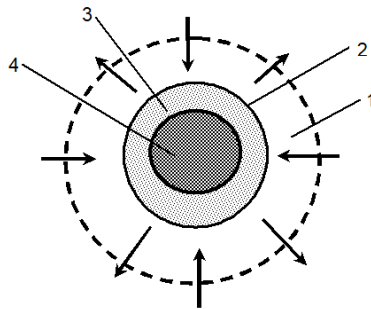
Burning liquid fuel is only possible due to the flame, which is then pre-sprayed into small droplets. Several factors can affect the combustion process, including the combustion chamber design, the oxygen concentration of the supplied air, and the injection pressure. The combustion of liquid fuel involves multiple stages.

The first stage involves heating the liquid fuel to boiling point and vaporizing it, followed by combustion in the second stage. Figure 2 illustrates how liquid fuel droplets burn. The fuel's combustion process occurs first after the droplets start vaporizing since their boiling point is lower than the ignition temperature. The combustion surface is penetrated by air through the resulting combustion products. The combustion rate is dependent on the size of the combustion surface, which is dependent on the degree of atomization of the liquid fuel. The greater the degree of atomization, the faster and more complete the combustion process.

A combustion zone is created near the droplet by the spherical surface, which has a diameter that is 1-5 times larger than the droplet's size. The droplet evaporates as a result of radiation heat from the combustion zone. Liquid fuel vapors and combustion products exist in the space between the droplet and the combustion zone. Air and combustion products can be found outside of the combustion zone. Fuel vapors are diffused into the combustion zone from the interior, and oxygen from the exterior. The chemical reaction is initiated by these components, which is followed by the release of heat and the formation of combustion products [19].

The cylindrical combustion chamber is 15 cm high and 4 cm in diameter (Fig.3). As depicted in Figure 4, the combustion chamber's general form is shown. The calculation space comprises of 600 cells. The fuel burns at 4 ms. The combustion chamber is filled with liquid fuel through a circular nozzle embedded in the middle of the chamber's lower part. The fuel droplet injection takes 1.4 ms to complete. Fuel injection speed is 250 m/s. Rapid

vaporization of the fuel after injection leads to combustion in the gas phase.



1 – oxidant and combustion products dissemination zone,  
2 – liquid, 3 – fuel vapor, 4 – liquid droplet

**Figure 2** – Liquid fuel's single droplet combustion plot

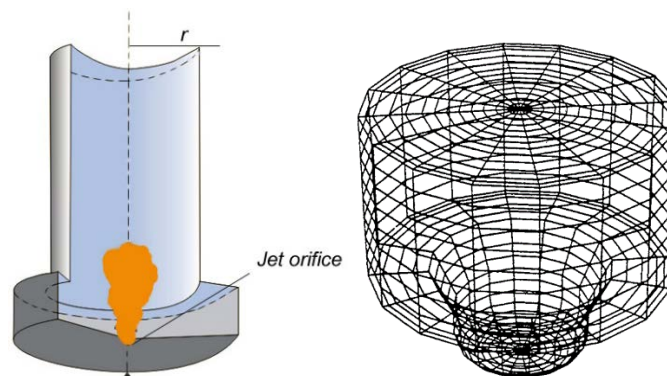


**Figure 3** – The combustion chamber's computer model and the prospect of the computing mesh created from the OFFSET option

#### 4 Modeling results

The work's objective is to investigate the liquid fuel injection speed impact on combustion by applying computer modeling techniques that solve for the differential equations of complex turbulent flows. The speed of how the liquid fuels were put into the chamber went from 150 to 350 m/s. Figure 4 displays how the flame temperature changes when the injecting liquid fuel droplets' speed is increased. The research focused on the fuel's injection rate and its influence on the maximum temperature achieved during the burning process. At speeds below 150 m/s, liquid fuels fail to ignite due to insufficient injection speed.

The most efficient combustion process of petrol occurs at the fuel injection speed of 200 m/s; at this time the temperature in the chamber takes the value of 2417 K. The effective speed of heptane is 250

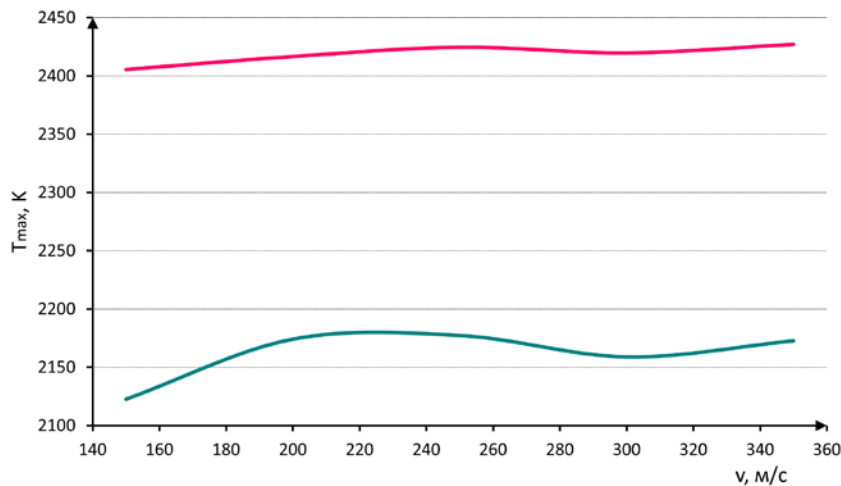
The wall's temperature in the combustion chamber is 353 K. The chamber's initial gas temperature is approximately 900 K. 300 K is the injected fuel's temperature. The injected droplets' initial radius is 3  $\mu\text{m}$ . The angle for droplet injection is 10 degrees.

Figure 3 also shows an axisymmetric structured computational grid used when conducting a numerical experiment in 3D modeling. The chamber's three-dimensional geometry is implemented by the SETUP subroutine by reading the initial design data using the OFFSET input option, considering the actual dimensions of the combustion chamber [10, 14, 20].

m/s. The maximum temperature at a given heptane droplet injection rate is 2177 K. Heptane's maximum gas temperature in the combustion chamber and the amount of carbon dioxide produced from burning the fuel depending on how fast the droplets are injected. At these injection rates, the fuel burns without residue, the concentration of produced  $\text{CO}_2$  is the lowest (Fig.5), and the chamber becomes extremely heated.

The graph in Figure 5 illustrates the correlation between the injection speed of petrol and heptane and the amount of carbon dioxide released in the combustion chamber. For petrol, at the optimum injection speed of 200 m/s, the concentration of  $\text{CO}_2$  produced is minimal, its value was 0.182 g/g. And at the combustion of heptane much less greenhouse gas is emitted (0.127 g/g) in comparison with petrol, which is an indicator of good calorific value of fuel, high mobility of its droplets, and active reacting chemical medium.





**Figure 4** – Change in the maximum combustion temperature of liquid fuel droplets with an increase in their injection rate: red line – petrol, green line – heptane

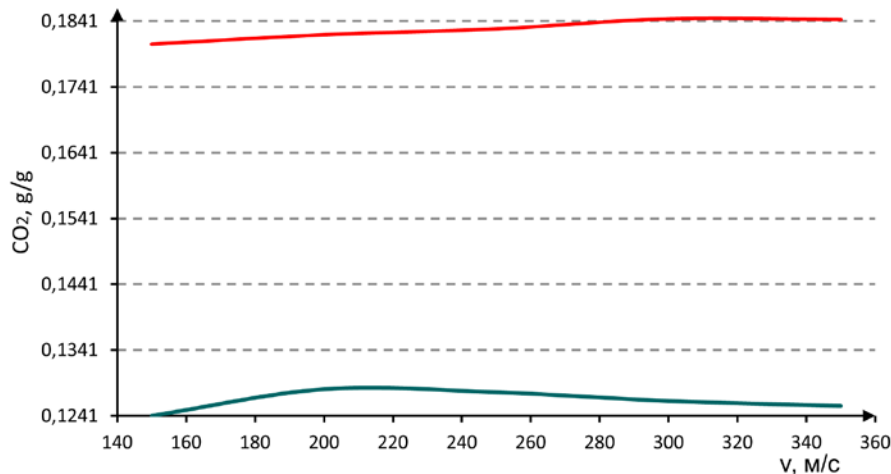


**Figure 5** – Effect of liquid fuel droplet injection rate on carbon dioxide  $CO_2$  distribution: red line – petrol, green line – heptane

Figures 6-14 exhibit the computer simulation results showing how liquid fuel burns in the chamber with droplets moving at an optimum speed.

Figures 6 and 7 demonstrate the liquid fuel droplets spread in the combustion chamber when it's injected at the proper speed. Flow visualization is presented at different time moments.

Analyzing the particle dispersion in Figures 6 and 7, during the combustion process, petrol droplets are concentrated at a 2 cm height in the combustion chamber, and heptane droplets up to 1 cm. Since heptane has a high surface tension, this affects the mobility and active reaction of its droplets with the oxidizing medium. In this regard,

it's safe to say that petrol droplets occupy a larger chamber area compared to heptane.

Similar distribution patterns of liquid fuel droplets (octane and dodecane) were observed by the authors in their studies [21-23]. Small fuel droplets and high levels of turbulence were determined to result in improved mixing with the oxidizer. This leads to plasma-chemical reactions taking place throughout the interior of the combustion chamber. These high-temperature energy processes are associated with the creation of environmentally friendly, energy-efficient, and energy-saving fuel technologies with minimal anthropogenic influence.

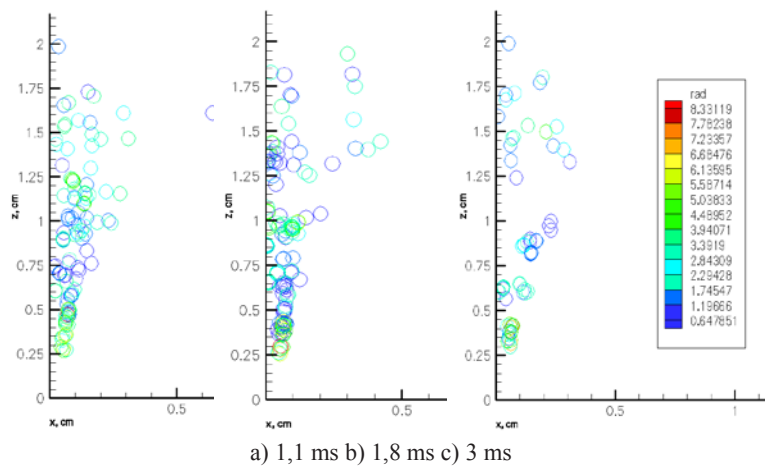


**Figure 6** –The petrol droplets dispersion by size at optimum injection speed 200 m/s

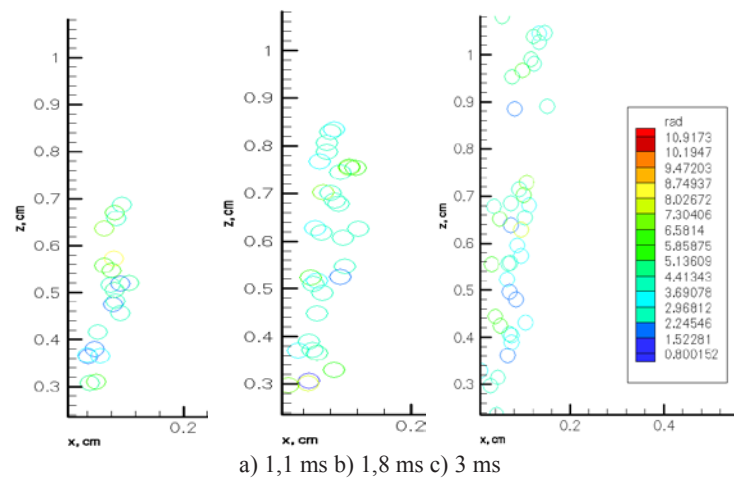


**Figure 7** – The heptane droplets dispersion by size at optimum injection speed 250 m/s

Figures 8 and 9 illustrate the fluctuation in peak temperatures for petrol and heptane in the combustion chamber at various time intervals. The graph in Figure 8 demonstrates the fluctuations in temperature within the fuel chamber for petrol. The hottest spot in the flame, which is at the center, reaches 3.6 cm high in the combustion chamber. The temperature in the remaining part of the chamber rises to 1133 K. Petrol can withstand temperatures of up to 2427 K while heptane can tolerate temperatures of up to 2177 K. Since the core of the heptane flare is at a chamber height of 4.2 cm.

Thus, with optimal temperature and speed of injected droplets, as well as rational combustion and proper organization of this process, it is conceivable to reduce the formation of such intermediate

reaction products as carbon monoxide and soot, which greatly harm the operation of the thermal engine [24].

Graphs 10 and 11 illustrate the fluctuations in carbon dioxide concentration at different altitudes within a combustion chamber while burning petrol and heptane. Up to 1.8 ms, no carbon dioxide is formed and the combustion process does not occur. While the  $\text{CO}_2$  concentration for petrol is 0.012 g/g at the initial time of 1.8 ms, during the last 4 ms of combustion time its value reaches up to 0.182 g/g. The combustion products reach their maximum values in the central part of the flare, also the maximum temperature values are observed here. The quantity of carbon dioxide formed during heptane combustion was 0.127 g/g.

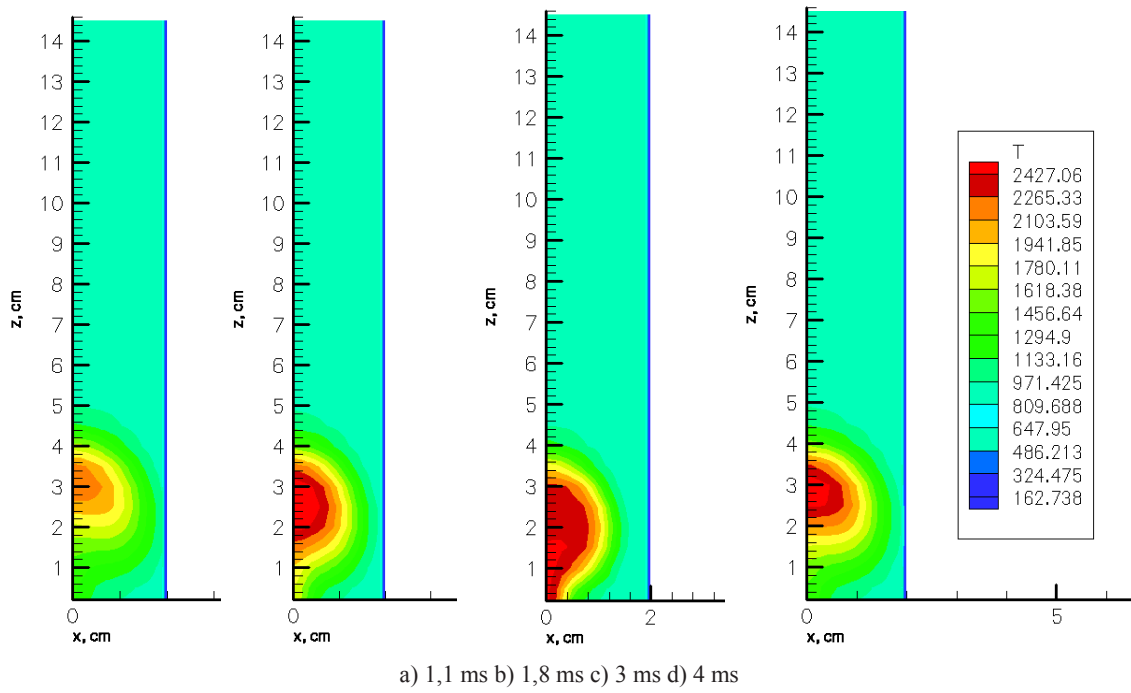


Figure 8 – Temperature profile during petrol combustion at different moments of time

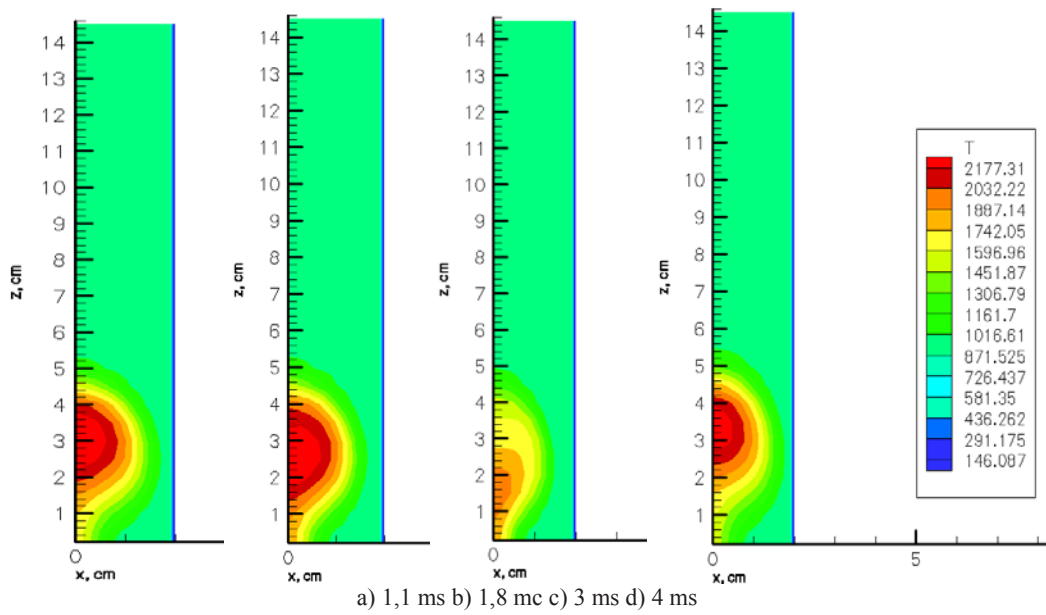


Figure 9 – Temperature profile during heptane combustion at different moments of time



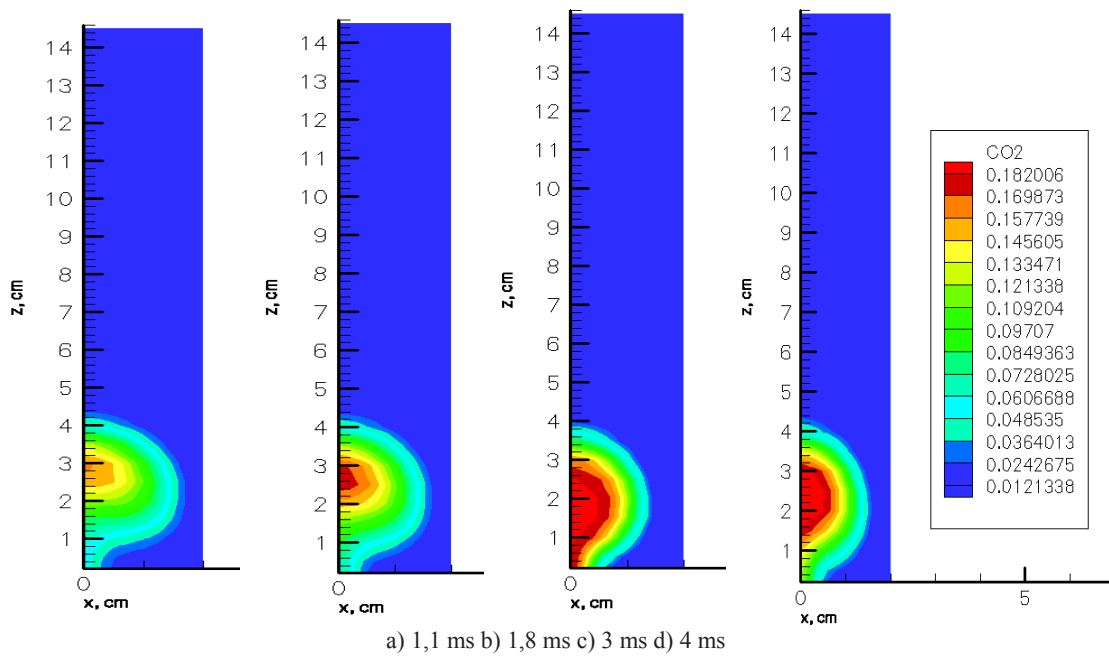


Figure 10 – Changes in CO<sub>2</sub> concentration fields during petrol combustion at different moments of time

Figures 12-13 show the change in nitrogen concentration with time. The highest amount of CO<sub>2</sub> changes at 1.5 ms. This time, the fuel is fully put into the combustion chamber, turned into vapor, and the chemical reaction starts.

In Figure 14, the rate at which the gas is moving in the combustion chamber is shown after 0.5 ms

during two different types of fuel (petrol and heptane) combustion. Petrol droplets are injected into the chamber at a speed of 200 m/s, and the gas inside the chamber is stationary, after injection liquid particles entrain the gas and acquire some speed, the graph of which is shown in Figure 14, a.

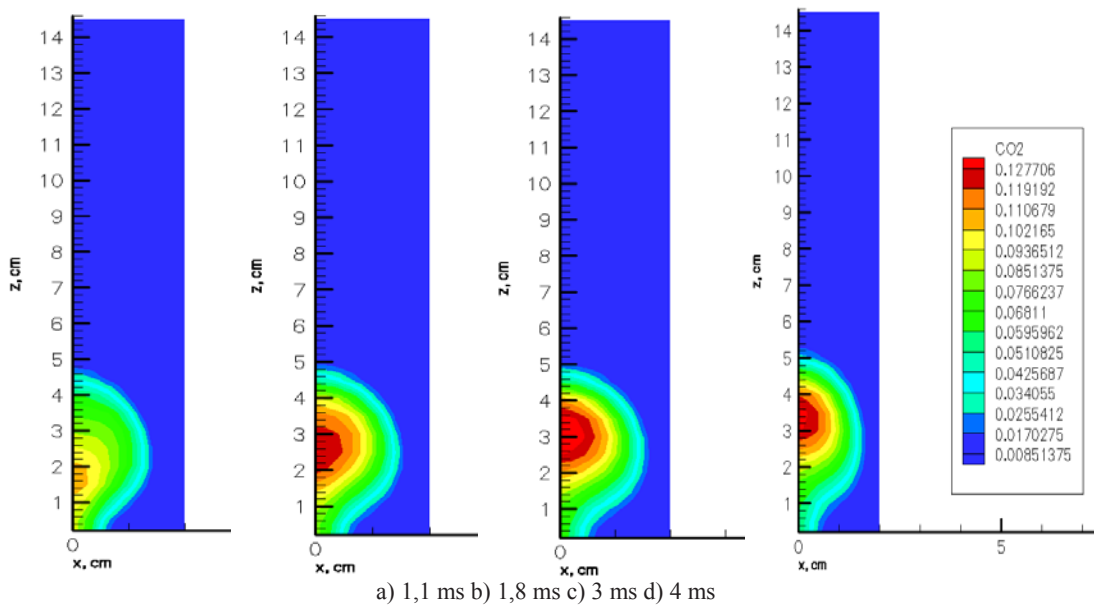


Figure 11 – Changes in CO<sub>2</sub> concentration fields during heptane combustion at different time moments

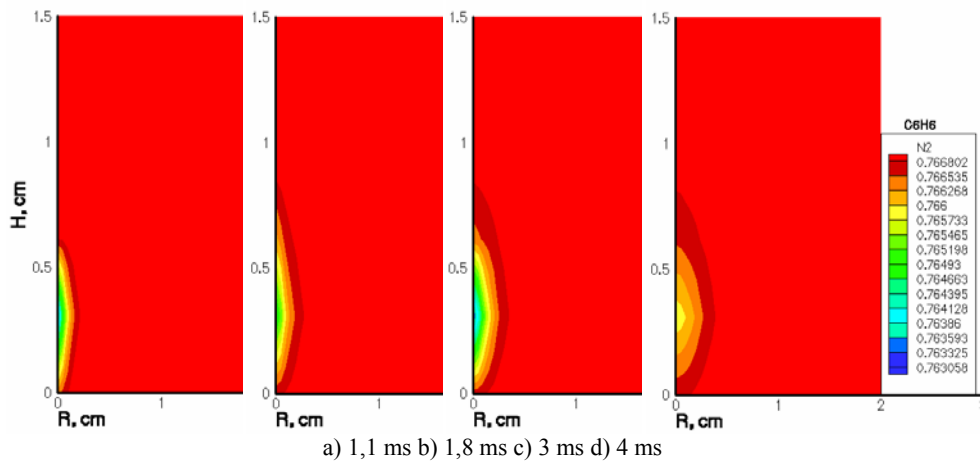


Figure 12 – Nitrogen concentration distribution during petrol combustion at different time moments

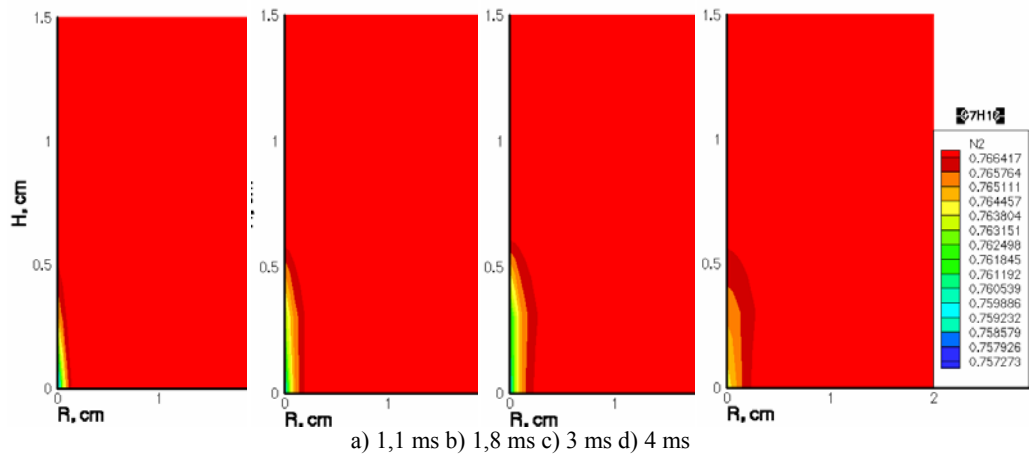


Figure 13 – Nitrogen concentration distribution during heptane combustion at different time moments

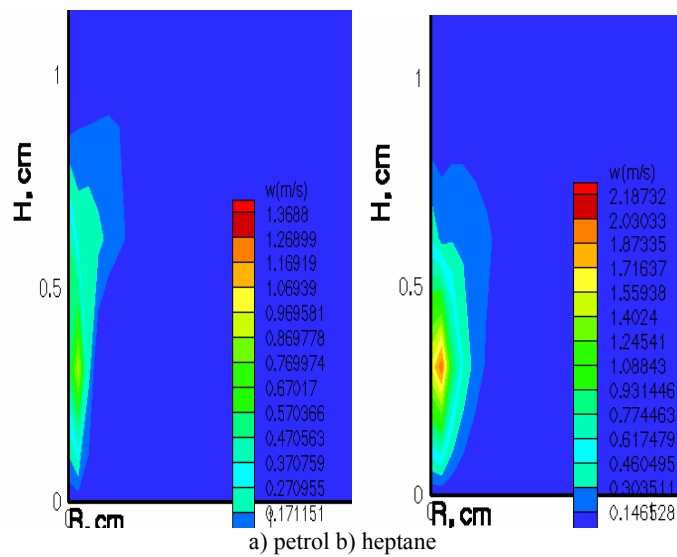


Figure 14 – Speed distribution in the combustion chamber during petrol and heptane combustion

The highest speed is observed in the middle of the combustion chamber, at a distance of about 1 cm from the center. Figure 14, b presents the results of speed calculations of heptane droplets in the combustion chamber at the same moment as for petrol. The optimum heptane droplet rate was 250 m/s.

## 5 Conclusions

This research focuses on understanding the combustion mechanisms of two different types of liquid fuel. It endeavors to find the most favorable air dynamics during turbulence and utilizes mathematical analysis to assess carbon dioxide generation in the combustion chamber.

When the injection speed is less than 200 m/s, there is no combustion because the speed is not fast enough to start and maintain the burning process. The optimum injection speed for liquid petrol is 200 m/s, while heptane is 250 m/s. As the fuel is ignited, the temperature inside the combustion chamber increases due to the accelerated spraying of fuel droplets.

How the distribution of specific chemicals and the temperature in the combustion chamber varies for two different fuels were determined. The liquid fuels combustion results in the creation of carbon

dioxide, leading to a rise in temperature within the combustion chamber and a faster burning of the fuel.

The use of computer models in studying the impact of turbulence on the dispersion of liquid particles in fuel combustion reveals an increased spread of fuel droplets. The combustion process is enhanced by the increased mixing area for fuel and air.

Our research findings can contribute to enhancing the efficiency of internal combustion engines. This will assist in increasing fuel efficiency and reducing detrimental emissions.

The application of the obtained optimal parameters in real thermal and technological installations will reduce the anthropogenic load on the surrounding atmosphere, which grows with the intensity of greenhouse gas emissions. Such methods of decarbonization in the energy sector contribute to the full implementation of sustainable global development goals.

## Acknowledgments

The Ministry of Science and Higher Education of Kazakhstan of the Republic of Kazakhstan No. AP14870834 has supported financially this work.

## References

1. Karaşan A., Gündoğdu F.K., Işık G., Kaya I., İlbarhar E. Assessment of governmental strategies for sustainable environment regarding greenhouse gas emission reduction under uncertainty // *Journal of Environmental Management*. – 2024. – Vol. 349, No. 119577. <https://doi.org/10.1016/j.jenvman.2023.119577>
2. Fayyazbakhsh A., Bell M.L., Zhu X., Mei X., Koutný M., Hajinajaf N., Zhang Y. Engine emissions with air pollutants and greenhouse gases and their control technologies // *Journal of Cleaner Production*. – 2022. – Vol. 376, No. 134260. <https://doi.org/10.1016/j.jclepro.2022.134260>
3. Wang L., Liu Y., Bi G., Zhang L., Song J. A phenomenological model of diesel combustion characteristics under CO<sub>2</sub>/O<sub>2</sub> atmosphere // *Fuel Processing Technology*. – 2022. – Vol. 229, No. 107167. <https://doi.org/10.1016/j.fuproc.2022.107167>
4. International Energy Agency report, 2023.
5. Report of the Agency for strategic planning and reforms of the Republic of Kazakhstan: On the state of protection of atmospheric air in the Republic of Kazakhstan, 2023.
6. Wang X., Zheng H., Wang Zh., Shan Yu., Meng J., Liang X., Feng K., Guan D. Kazakhstan's CO<sub>2</sub> emissions in the post-Kyoto Protocol era: Production-and consumption-based analysis // *Journal of Environmental Management*. – 2019. – Vol. 249, No. 109393. <https://doi.org/10.1016/j.jenvman.2019.109393>
7. Obiora S.Ch., Bamisile O., Hu Y., Ozsahin D.U., Adun H. Assessing the decarbonization of electricity generation in major emitting countries by 2030 and 2050: Transition to a high share renewable energy mix // *Heliyon*. – 2024. – Vol.10, Issue 8, No. e28770. <https://doi.org/10.1016/j.heliyon.2024.e28770>
8. Addai K., Serener B., Kirikkaleli D. Complementarities in the effect of economic globalization and decarbonization technologies on carbon neutrality. Evidence from Germany using Fourier-based approaches // *World Development Sustainability*. – 2023. – Vol. 3, No. 100050. <https://doi.org/10.1016/j.wds.2023.100050>
9. Shirzadi M., Tominaga Yo. Computational fluid dynamics analysis of pollutant dispersion around a high-rise building: Impact of surrounding buildings // *Building and Environment*. – 2023. – Vol. 245, No. 110895. <https://doi.org/10.1016/j.buildenv.2023.110895>
10. Amsden A.A. Kiva-3v, release 2, improvements to kiva-3v. Los Alamos, 1999. – 34 p.

11. Gorokhovski M., Hermann M. Modeling primary atomization // *Annual Review of Fluid Mechanics*. – 2008. – Vol. 40. – P. 343–366. <https://doi.org/10.1146/annurev.fluid.40.111406.102200>
12. Amsden A.A., O'Rourke P.J., Butler T.D. KIVA-II: A computer program for chemically reactive flows with sprays. Los Alamos, 1989. – 160 p.
13. Gorokhovski M.A., Oruganti S.K. Stochastic models for the droplet motion and evaporation in under-resolved turbulent flows at a large Reynolds number // *Journal of Fluid Mechanics*. 2022. – Vol. 932, No. A18. <https://doi.org/10.1017/jfm.2021.916>
14. Amsden A.A. KIVA-3: A KIVA Program with block-structured mesh for complex geometries. Los Alamos, 1993. – 95 p.
15. Mok M.Ch., Yeoh Ch.V., Tan M.K., Foo J.J. Optimization of Reynolds stress model coefficients at multiple discrete flow regions for three-dimensional realizations of fractal-generated turbulence // *European Journal of Mechanics – B/Fluids*. – 2024. – Vol. 106. – P. 30–47. <https://doi.org/10.1016/j.euromechflu.2024.03.002>
16. Zhao Y., Akolekar H.D., Weatheritt J., Michelassi V., Sandberg R.D. RANS turbulence model development using CFD-driven machine learning // *Journal of Computational Physics*. – 2020. – Vol. 411, No. 109413. <https://doi.org/10.1016/j.jcp.2020.109413>
17. Gao N., Niu J., He Q., Zhu T., Wu J. Using RANS turbulence models and Lagrangian approach to predict particle deposition in turbulent channel flows // *Building and Environment*. – 2012. – Vol. 48. – P. 206–214. <https://doi.org/10.1016/j.buildenv.2011.09.003>
18. Bolegenova S., Askarova A., Slavinskaya N., Ospanova Sh., Maxutkhanova A., Aldiyarova A., Yerbosynov D. Statistical modeling of spray formation, combustion, and evaporation of liquid fuel droplets // *Physical Sciences and Technology*. – 2022. – Vol. 9, No. 3-4. – P. 69–82. <https://doi.org/10.26577/phst.2022.v9.i2.09>
19. Bhoite S., Windom B., Singh J., Montgomery D., Marchese A.J. A study of ignition and combustion of liquid hydrocarbon droplets in premixed fuel/air mixtures in a rapid compression machine // *Proceedings of the Combustion Institute*. – 2023. – Vol. 339, Issue 2. – P. 2533–2542 <https://doi.org/10.1016/j.proci.2022.08.125>
20. Maghbouli A., Yang W., An H., Li J., Chou S.K., Chua K.J. An advanced combustion model coupled with detailed chemical reaction mechanism for D.I diesel engine simulation // *Applied Energy*. – 2013. – Vol. 111. – P. 758–770. <https://doi.org/10.1016/j.apenergy.2013.05.031>
21. Berezovskaya I.E., Tasmukhanova A.A., Ryspaeva M.Zh., Ospanova Sh.S. Investigation of the influence of liquid fuel injection rate on the combustion process using KIVA-II software // *Eurasian Physical Technical Journal*. – 2023. – Vol. 20, Issue 3 (45). – P. 43–51. <https://doi.org/10.31489/2023No3/43-51>
22. Askarova A., Bolegenova S., Ospanova Sh., Rakhimzhanova L., Nurmukhanova A., Adilbayev N. Optimization of fuel droplet sputtering and combustion at high turbulence flows // *Russian Physics Journal*. – 2024. – Vol. 67, Issue 2. – P. 167–170. <https://doi.org/10.1007/s11182-024-03104-5>
23. Askarova A., Bolegenova S., Ospanova Sh., Slavinskaya N., Aldiyarova A., Ungarova N. Simulation of non-isothermal liquid sprays under large-scale turbulence // *Physical Sciences and Technologies*. – 2021. – Vol 8, No. 3-4. – P. 28–40. <https://doi.org/10.26577/phst.2021.v8.i2.04>
24. Askarova A., Bolegenova S., Mazhrenova N., Manatbayev R., Ospanova Sh., Bolegenova S., Berezovskaya I., Maximov V., Nugymanova A., Shortanbayeva Zh. 3D modelling of heat and mass transfer processes during the combustion of liquid fuel // *Bulgarian Chemical Communications*. – 2016. – Vol. 48, Issue E. – P. 229–235.

**Information about authors:**

*Bolegenova Saltanat, Doctor of Physical and Mathematical Sciences, is a Professor at the al-Farabi Kazakh National University (Almaty, Kazakhstan), e-mail: Saltanat.Bolegenova@kaznu.edu.kz;*

*Askarova Aliya, Doctor of Physical and Mathematical Sciences, is a Professor at the al-Farabi Kazakh National University (Almaty, Kazakhstan), e-mail: Aliya.Askarova@kaznu.edu.kz;*

*Ospanova Shynar (corresponding author), PhD, is a Senior Lecturer at the al-Farabi Kazakh National University (Almaty, Kazakhstan), e-mail: Shynar.Ospanova@kaznu.edu.kz;*

*Zhumagaliyeva Sabina, Master student at the al-Farabi Kazakh National University (Almaty, Kazakhstan), e-mail: zhumasabina@icloud.com;*

*Makanova Ayaulym, Master student at the al-Farabi Kazakh National University (Almaty, Kazakhstan), e-mail: aiko.20.20@mail.ru;*

*Aldiyarova Aliya is a Lecturer at the al-Farabi Kazakh National University (Almaty, Kazakhstan), e-mail: aliya.aldiyarova14@gmail.com;*

*Nurmukhanova Alfiya, Candidate of Technical Sciences, is Senior Lecturer at the al-Farabi Kazakh National University (Almaty, Kazakhstan), e-mail: alfiyanurmukhanova7@gmail.com;*

*Idrissova Gulzhan, is a Senior Lecturer at the al-Farabi Kazakh National University (Almaty, Kazakhstan), e-mail: alikosh.bekbayev@gmail.com*